frontiers | Frontiers in Earth Science

TYPE Original Research
PUBLISHED 06 June 2024
DOI 10.3389/feart.2024.1402922

OPEN ACCESS

EDITED BY
Junrong Zhang,
China University of Geosciences
Wuhan, China

REVIEWED BY
Bocheng Zhang,
China University of Geosciences
Wuhan, China
Aiguo Xing,
Shanghai Jiao Tong University, China
Tao Wen,
Yangtze University, China

*CORRESPONDENCE
Ping Wang,
wangping@gsdzj.gov.cn

RECEIVED 18 March 2024
ACCEPTED 07 May 2024
PUBLISHED 06 June 2024

CITATION
Wang Y, Wang P, Chang W, Wang H, Xu S, Xu S and Yu H (2024), Hazard assessment of seismic-collapsed loess landslides on the Loess Plateau as exemplified by the M6.2 earthquake in Jishishan County, China. *Front. Earth Sci.* 12:1402922. doi: 10.3389/feart.2024.1402922

Hazard assessment of seismic-collapsed loess landslides on the Loess Plateau as exemplified by the M6.2 earthquake in Jishishan County, China

Yali Wang[1,2], Ping Wang[1,2]*, Wenbin Chang[3], Huijuan Wang[1,2], Shiyang Xu[1,2,4], Shuya Xu[5] and Haoran Yu[1,2]

[1]Lanzhou Institute of Seismology, China Earthquake Administration, Lanzhou, China, [2]Key Laboratory of Loess Earthquake Engineering, China Earthquake Administration, Lanzhou, China, [3]State Key Laboratory of Ocean Engineering, Shanghai Jiao Tong University, Shanghai, China, [4]Key Laboratory of Earthquake Engineering and Engineering Vibration of China Earthquake Administration, Institute of Engineering Mechanics, China Earthquake Administration, Harbin, Heilongjiang, China, [5]Geophysical Exploration Center, China Earthquake Administration, Zhengzhou, China

The Loess Plateau is marked by intense neotectonic activity and frequent earthquakes. Its unique physico-mechanical properties, combined with the granular overhead pore structure of loess, render it prone to seismic landslides triggered by strong earthquakes. Different types of loess seismic landslides have distinct formation mechanisms, disaster-causing characteristics, and risk assessment programs. In this study, the risk of seismic-collapsed loess landslides as one of the types of loess seismic landslides was evaluated on the Loess Plateau. A risk zoning map for seismic-collapsed loess landslides on the Loess Plateau, considering various exceedance probabilities, was compiled by assessing eight factors. These factors include peak ground acceleration, microstructure of loess, and were evaluated using both the minimum disaster-causing seismic peak ground acceleration zoning method and the analytic hierarchy process. The following conclusions were obtained: (1) Earthquakes are the primary inducing factor for seismic-collapsed loess landslides, with other factors serving as influencers, among which the microstructure of loess carries the highest weight; (2) Across various exceedance probabilities, the likelihood of seismic-collapsed loess landslides occurring at 63% of the 50-year exceedance probability is low. Moreover, as the minimum hazard-causing seismic peak ground acceleration increases, the risk of occurrence of seismic-collapsed loess landslides rises, leading to a gradual expansion of the area share in moderate and high-risk zones; (3) Hazard evaluation results align well with existing data on seismic-collapsed loess landslides and findings from field investigations. The case of seismic-collapsed loess landslides induced by the M6.2 magnitude earthquake in Jishishan County, China, is presented as an illustration. The combined use of the minimum hazard-causing seismic peak ground acceleration zoning method and the analytic hierarchy process method offers a reference for geohazard hazard

assessment, with earthquakes as the primary inducing factor and other factors as influencers.

KEYWORDS

geographic information system (GIS), loess subsidence, loess seismic landslides, seismic-collapsed loess landslides, minimum hazard-causing seismic peak ground acceleration

1 Introduction

Loess is a Quaternary loose sediment with water sensitivity, earthquake vulnerability, and development of joints and fissures (Wang, 2003; Guo et al., 2023). The Loess Plateau constitutes the primary distribution area of loess in China, where seismic activity manifests as intense expressions of neotectonic movement. According to the statistics of the historical earthquake catalog, a total of 420 earthquakes with magnitudes equal to or greater than M≥4¾ have occurred on the Loess Plateau. These include major events such as the M=8¼ earthquake in Hua County in 1,556, the M=8.0 earthquake in Tianshui City in 1,654 and the M=8.0 earthquake in Gulang County in 1927 (Fang et al., 2023). These destructive earthquakes, combined with the significant ground vibration amplification effect of loess sites (Wang et al., 2017), have induced loess seismic disasters such as landslides, seismic subsidence, and liquefaction, resulting in casualties and substantial economic losses (Zhang et al., 2017). The major earthquakes can trigger clustered and widespread landslides covering thousands of square kilometer. A single loess layer liquefaction and slip zone can extend over several square kilometers, while seismic subsidence areas of several square kilometers can experience non-uniform subsidence of 2–3 m. As a result, casualties from these events can make up one-third to half of the total earthquake-related deaths, in addition to causing destruction of buildings and infrastructure (Wang, 2022).

Characteristics and destabilisation mechanisms of loess seismic landslides vary under seismic action. Loess seismic landslides can be mainly divided into three types: the shear-sliding type, seismic-collapsibility type, and liquefaction type (Figure 1) (Pu and Xu, 2019; Wang et al., 2023). Shear failure approximates the damage pattern of general soil landslides, with a complete and continuous shear sliding surface (Figure 1A). Seismic collapse failure is mainly caused by structural subsidence of loess, which manifests itself as vertical settlement of the loess site. According to the damage form of seismic subsidence, it can be divided into trap-slip type and collapse-slip type. In the diagram on the left side of Figure 1B, most of the sliding soil sits on the sliding surface and is of the trap-slip type. In the diagram on the right side of Figure 1B, most of the sliding soil falls below the foot of the slope and is of the collapse-slip type (Fang et al., 2023; Wang et al., 2023). Liquefaction failure is dominated by the development of soil shear contraction and pore water pressure, and the slip surface is gentle and has a long slip range (Figure 1C) (Zhang and Li, 2011). Different types of deformation damage-induced loess landslides have different distances of movement, extent of disaster, causal mechanisms, preventive measures against disasters, and different risk assessment programmes.

Seismic subsidence of loess is an abrupt additional subsidence of unsaturated loess under seismic loading (Qiu et al., 2018). Its formation is due to the very weak inter-particle cementation and low strength. By seismic action, the macroporous structure may be destroyed, and the powder particles fall into the macroporous space, so that the residual deformation of the loess layer grows rapidly (Xing et al., 2016). Induced by seismic subsidence of seismic-collapsed loess landslides, they are characterised by significant vertical settlement and deformation under seismic action, large ground cracks, relatively small travelling distances and disaster-causing ranges (Roslee et al., 2017). They also have gentle slope gradients, absence of groundwater action, and high sliding rates. Hazard zoning of seismic-collapsed loess landslides can provide a basis for disaster prevention and mitigation.

With the increasing frequency and intensity of earthquakes, the importance of seismic landslide hazard assessment is becoming increasingly prominent. The landslide hazard assessment programmes consists mainly of qualitative assessment methods, deterministic models and statistical analysis models: qualitative assessment is an empirical model, and common methods include the analytic hierarchy process (Myronidis et al., 2016; Basu and Pal, 2017); deterministic models require detailed spatial variable parameters, such as the Newmark model (Jin et al., 2019; Zang et al., 2019; Newmark, 1965), the SHALSTSAB model (Sun et al., 2021), the CSDI model (Zhang et al., 2024a); statistical analysis models require large amounts of data to obtain reliable results, such as logistic regression models (Bui et al., 2011; Aditian et al., 2018; Li et al., 2019). The morphology of seismic-collapsed loess landslides is strongly influenced by surface reconstruction, and it is difficult to obtain the number and characteristics of this landslide type through remote sensing interpretation and inversion analysis (Fang et al., 2023). Currently, there is no complete database of seismic-collapsed loess landslides, and data-driven statistical analyses and machine-learning methods with high requirements for sample set construction are not applicable for the time being (Shahabi et al., 2023; Zhang et al., 2024b; Li et al., 2024). The study selected the minimum hazard-causing seismic peak ground acceleration zoning method combined with the analytic hierarchy process. It used the minimum hazard-causing seismic peak ground acceleration, loess microstructure, degree of relief, slope, stratum, landform types, loess thickness, and average annual rainfall as the evaluation factors. Compiled a zoning map of the seismic-collapsed loess landslides on the Loess Plateau with different exceedance probabilities, i.e., under the basic ground motion, the rare ground motion, and the very rare ground motion. Historical data enquiries and field investigations were conducted. The site of seismic-collapsed loess landslides generated by the M6.2 magnitude earthquake in Jishishan County, Gansu Province, China, was used as the primary example.

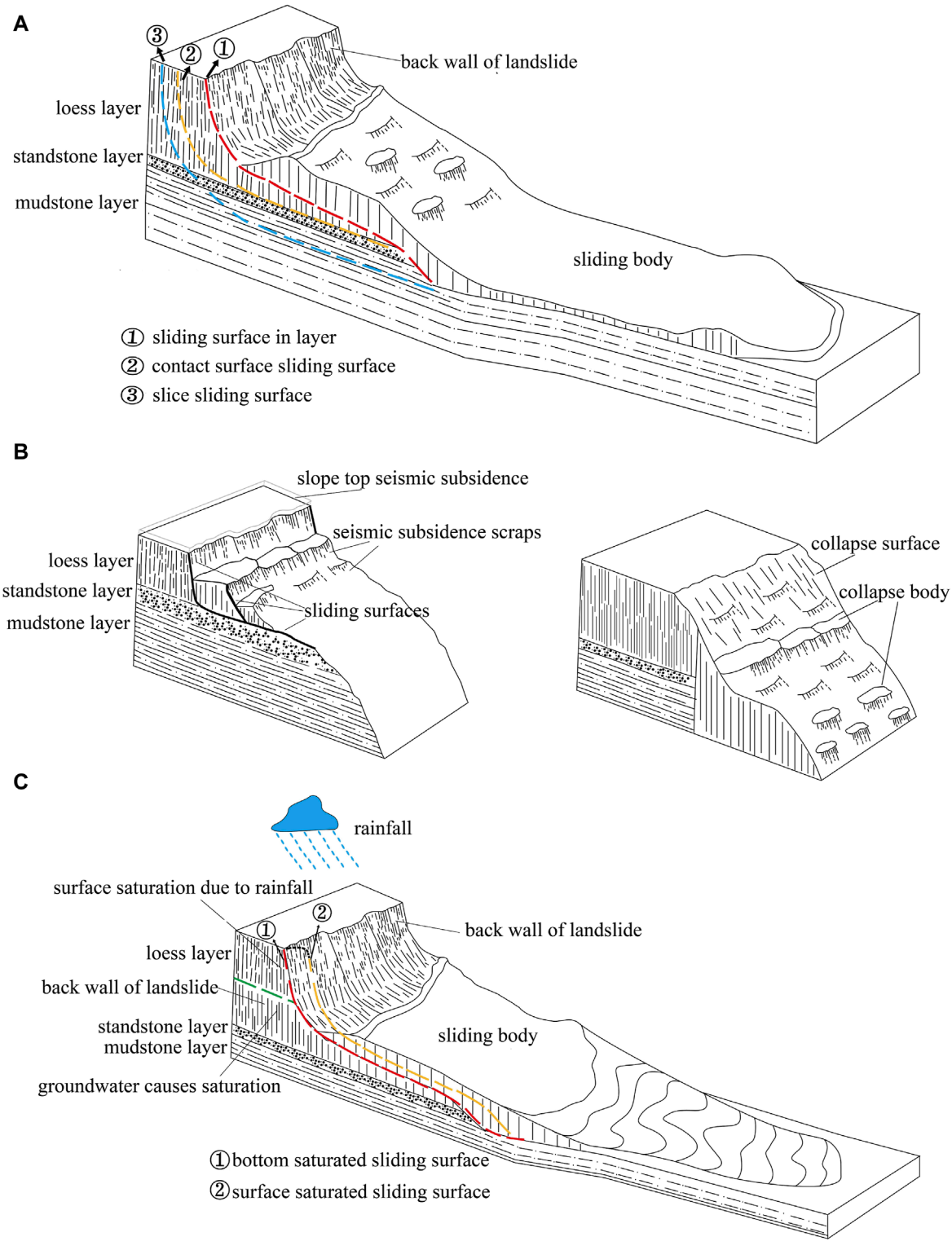

FIGURE 1
Schematic diagram of different types of loess seismic landslides: **(A)** Schematic diagram of shear-sliding loess landslide. **(B)** Schematic diagram of seismic-collapsed loess landslide. **(C)** Schematic diagram of liquefied loess landslide [modified from Wang et al. (2023)].

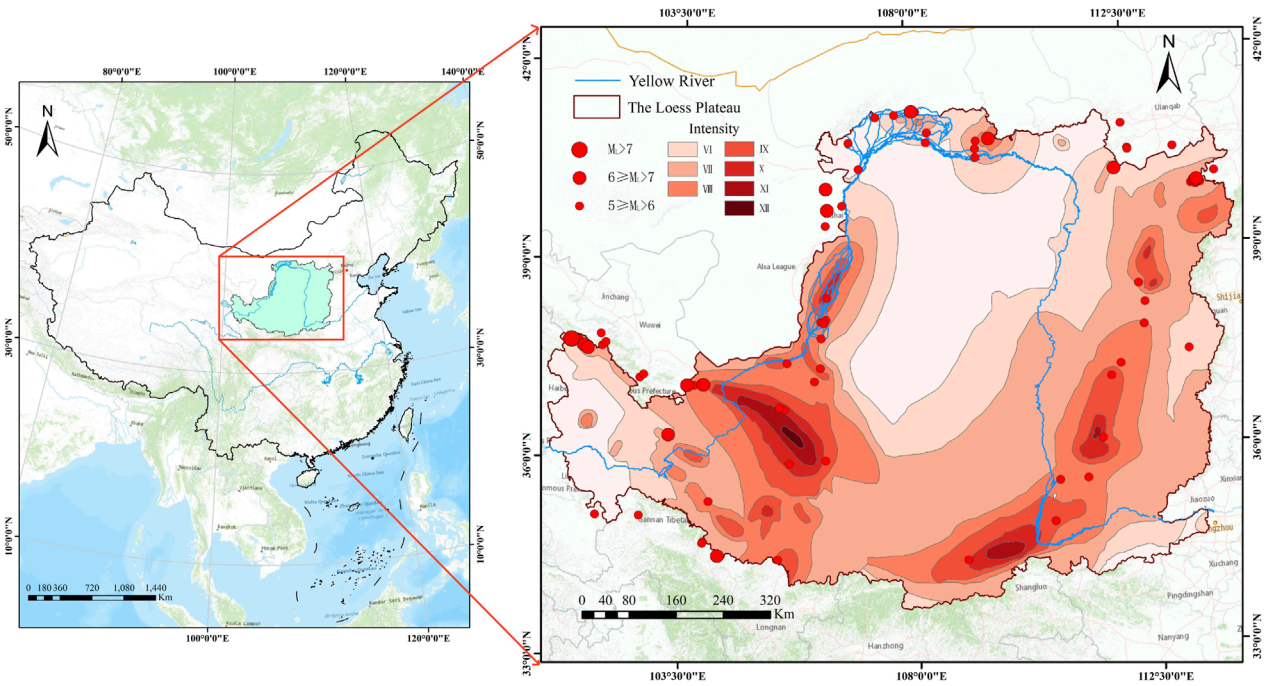

FIGURE 2
Loess Plateau Zone and Intensity Distribution Map. (refer to The Chinese seismic intensity scale. GB/T 17742–2020).

2 Study area and data sources

2.1 Study area

The Loess Plateau is located in the north of central China, and is the most concentrated and largest loess area in the world. The terrain is high in the northwest and low in the southeast. A variety of landforms have been formed under the action of geological structures, hydraulic erosion, wind transport and accumulation, and other internal and external forces of the earth. The Loess Plateau is characterised by a typical continental monsoon climate, with cold, dry winters and hot, stormy summers. The region is characterised by strong neotectonic movements, active crust and frequent earthquakes, with more than 50 earthquakes of magnitude 6.0 or higher and five earthquakes of magnitude eight or higher (Wang et al., 2023). More than 80% of the seismic events on the Loess Plateau occur in regions with a seismic intensity of VI or higher, with over half of them concentrated in zones VII and VIII (Figure 2) (Peng, 2019). The unique microstructure of loess renders it highly susceptible to seismic activity, leading to various seismic hazards such as landslides, subsidence, and liquefaction during successive strong earthquakes.

2.2 Data sources

The data used in this article contains: (1) 30 m resolution Digital Elevation Model (DEM), derived from Geospatial Data Cloud (https://www.gscloud.cn), the ArcGIS platform was processed to obtain degree of relief and slope factors. (2) Nationwide day-by-day precipitation data for 2012–2021. Sourced from the China Tibetan Plateau Science Data Centre (https://data.tpdc.ac.cn); average annual rainfall factors were obtained by processing on the ArcGIS platform. (3) The spatial extent of the Loess Plateau is derived from Resource and Environment Science and Data Center (https://www.resdc.cn). (4) Geological map of China 1:1 million. Sourced from GeoCloud (https://data.tpdc.ac.cn), the ArcGIS platform extracted to obtain the lithological factors of the Loess Plateau stratum.

3 Impact factor analysis for seismic-collapsed loess landslides

Factors influencing loess subsidence include physical indicators of loess (water content, dry density); mechanical properties (pore ratio, modulus of elasticity, consolidation pressure, shear wave velocity); seismic effects (intensity, type of loading, vibration frequency, predominant period, effective duration, peak intensity); microstructure of loess; stratigraphic structure; geomorphological features and so on (Duan and Zhang, 1990; Runde et al., 2007).

Influencing factors of loess seismic landslides include seismic factors; topographic and geomorphic factors (slope, slope direction, slope angle, slope of aspect, stratum, landform, distance from fault, thickness of coverage of the Loess layer); hydraulic factors (stream power index, topographic wetness index, distance from river); anthropogenic factors and so on (Wang et al., 2012; Wang, 2020; Zhong et al., 2022; Li et al., 2023). Due to differences in geological environment conditions in different study areas, the development and spatial distribution pattern of landslides in the

TABLE 1 Hazard-causing minimum intensities and PGA values for loess seismic hazards.

Type of disaster	PGA (gal)				Intensity (degrees)			
Sesmic landslide	170				7			
subsidence	I	II	III	IV	I	II	III	IV
	100	180	350	700	7	8	9	10
liquefaction	100				7			

region can vary significantly. Therefore, the factors listed above in the geological environment may not necessarily exert a significant impact on landslide development in the study area (Qian, 2023). The evaluation factors for seismic-collapsed loess landslides were selected by referencing factors for loess seismic landslides. This selection considered the main characteristics of loess subsidence, the availability of evaluation data across the Loess Plateau, and the simplicity, operability, and hierarchy of factor selection. Among the numerous factors, earthquakes were clearly identified as inducing factors in the risk assessment of seismic-collapsed loess landslides, while the rest were considered influencing factors. The eight factors of minimum hazard-causing seismic peak ground acceleration, microstructure of loess, topography and geomorphology (degree of relief, slope, stratum and landform types, loess thickness), and hydraulics (average annual rainfall) are selected as the evaluation factors for the seismic-collapsed loess landslides on the Loess Plateau.

3.1 Minimum hazard-causing seismic peak ground acceleration

The seismic peak ground acceleration (PGA) is a measure of seismic intensity (Wang et al., 2004). According to Newton's second law of motion, the relationship between force and acceleration of an object is expressed as $F=ma$, where m is the mass of the object and a is the acceleration. Thus, the greater the seismic peak ground acceleration, the stronger the seismic force on the object, leading to a greater risk of producing loess geological hazards such as subsidence, liquefaction, and landslides. Minimum hazard-causing seismic peak ground acceleration and maximum hazard-causing distance methods can be used as indicators for class I zoning of loess seismic hazards (Wang, 2003). According to Table 1 (Wang, 2003), the minimum hazard-causing PGA value for level I is 100 gal. Based on seismic ground motion parameter zonation map of China (GB 18306–2015), the minimum hazard-causing PGA value for level I to IV is normalised. The seismic peak ground acceleration is 0.1 g, which produces class I loess subsidence. A seismic peak ground acceleration of 0.17 g induces loess seismic landslides. Seismic peak ground acceleration of 0.2 g is critical for inducing seismic-collapsed loess landslides. Seismic peak ground acceleration of 0.2–0.4 g results in moderate seismic-collapsed loess landslides. Peak ground acceleration of 0.4–0.8 g leads to severe seismic-collapsed loess landslides, while >0.8 g induces very severe seismic-collapsed loess landslides. (Figure 3).

3.2 Loess microstructure

Loess possesses a granular shelf pore structure. Subsidence in loess occurs due to damage to its special pore microstructure, where particles infiltrate the pore space, leading to changes in the volume of the soil body and resulting in macroscopic soil subsidence. At the same time, loess subsidence is closely related to microstructural parameters such as the radius of shelf space of loess particles (r), the maximum pore radius (r_{max}), the initial porosity (n_0), and the distribution pattern of shelf space of the soil ($N(r)$) (Formula 1) (Shi and Qiu, 2011; Xu et al., 2021).

$$\Delta V = \Delta V_1 + \Delta V_2 = \int_{r_0}^{r_{max}} 2n_0 N(r)\left(r^2 - r_0^2\right)dr + \int_0^{R_0} \pi R^2 (1-n_0) N(R) e^{-\frac{R}{R_0}} dR \quad (1)$$

Where ΔV is the change in volume of loess after loess subsidence when the total volume of the soil is taken as 1. ΔV_1 is the volume of the soil damaged due to the change of shelf pores in the microstructural damage of loess, and ΔV_2 is the total volume of nucleated particles in the microstructural damage of loess. r_0 is the minimum radius that destroys the shelf pore, R is the nucleated particle size, R_0 is the nucleated maximum particle size, and N(R) is the particle probability distribution curve.

The formation of loess reflects the regional character of monsoon action, with different microstructural features formed under different climatic conditions (Wang and Deng, 2023). Based on Deng et al.'s classification of microstructural types of loess in the central and western regions, an overview of the microstructural distribution on the Loess Plateau was extracted, as depicted in Figure 4A (Deng et al., 2003). The classification criteria are detailed in Table 2, where Class III exhibits the strongest seismic trapping propensity, while Class V demonstrates the weakest seismic trapping propensity.

3.3 Degree of relief

The greater the degree of relief, the greater the change in terrain within a given area. Landslides are prone to occur in areas of intense topographic change. The degree of relief of the Loess Plateau ranges from 0 to 731 m (Figure 5A), with the largest degree of relief being 731 m, which is a higher degree of relief, consistent with the geomorphological pattern of the Loess Plateau with its thousands of gorges and ravines. We selected the concentrated distribution areas of loess seismic landslides: Tianshui City, Tongwei County,

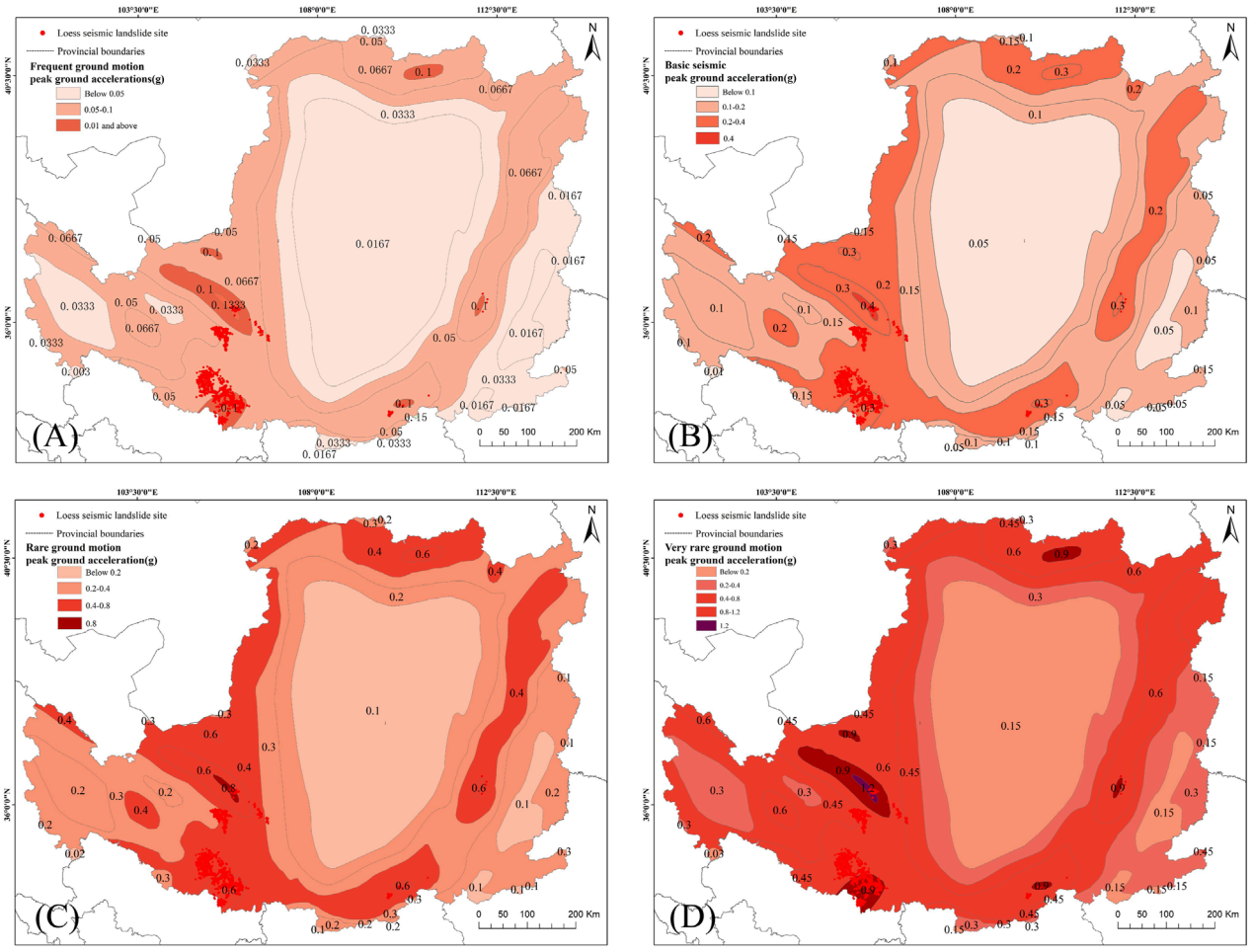

FIGURE 3
Seismic ground motion parameters zonation map of the Loess Plateau: **(A)** Zoning map of frequent ground motion parameters. **(B)** Zoning map of basic ground vibration parameters. **(C)** Zoning map of rare ground motion parameters. **(D)** Zoning map of very rare ground motion parameters. (refer to seismic ground motion parameters zonation map of China).

and Xiji County. Then, we analyzed the relationship between the degree of relief and the number of landslides, as well as the number density of landslides (LND) across different classification intervals (Figure 5B) (Tian et al., 2016). We found the proportion of landslides in the range of 100–150 m was highest, and the relationship between the degree of relief and the proportion of landslides basically conformed to a normal distribution. At the same time, the number of landslides in Tianshui City and Tongwei County and the LND have the same trend in the classification interval. The highest number of landslides in the range of 100–150 m, and a dense spatial distribution of landslides in the range of 150–200 m.

3.4 Slope

The original slope angles of seismic-collapsed loess landslides were in the range of 5°–15° (Wang, 2003). According to the slope distribution map of the Loess Plateau (Figure 5C), the statistics of loess seismic landslides densely distributed in Xiji County, Tongwei County, and Tianshui City. The number of landslides in the three areas as well as the percentage of the number of landslides showed a consistent trend under the same slope grading interval. Landslides are most prevalent within the 5°–15° range, while the least occurrences are found within the 0°–5° and >30° ranges, indicating that slope which are particularly gentle as well as overly steep are less conducive to landslide disasters. At the same time, loess seismic landslides have no obvious pattern in the spatial distribution under different slope classifications (Figure 5D).

3.5 Stratum and landform types

Loess is an accumulation since the Quaternary and is divided into Early Pleistocene palaeo loess (Q_1), Middle Pleistocene old loess (Q_2), Late Pleistocene neo loess (Q_3) and Holocene recent loess (Q_4) according to the epoch in which it was formed. Compared with Q_1 and Q_2 loess, Q_3 and Q_4 loess is more recent, with large pores, vertical joints, loose structure, and poorer seismic resistance, loess subsidence mainly occurs in Q_3 and Q_4 stratum (Figure 4B) (Wang, 2003). Holocene and Late Pleistocene loess

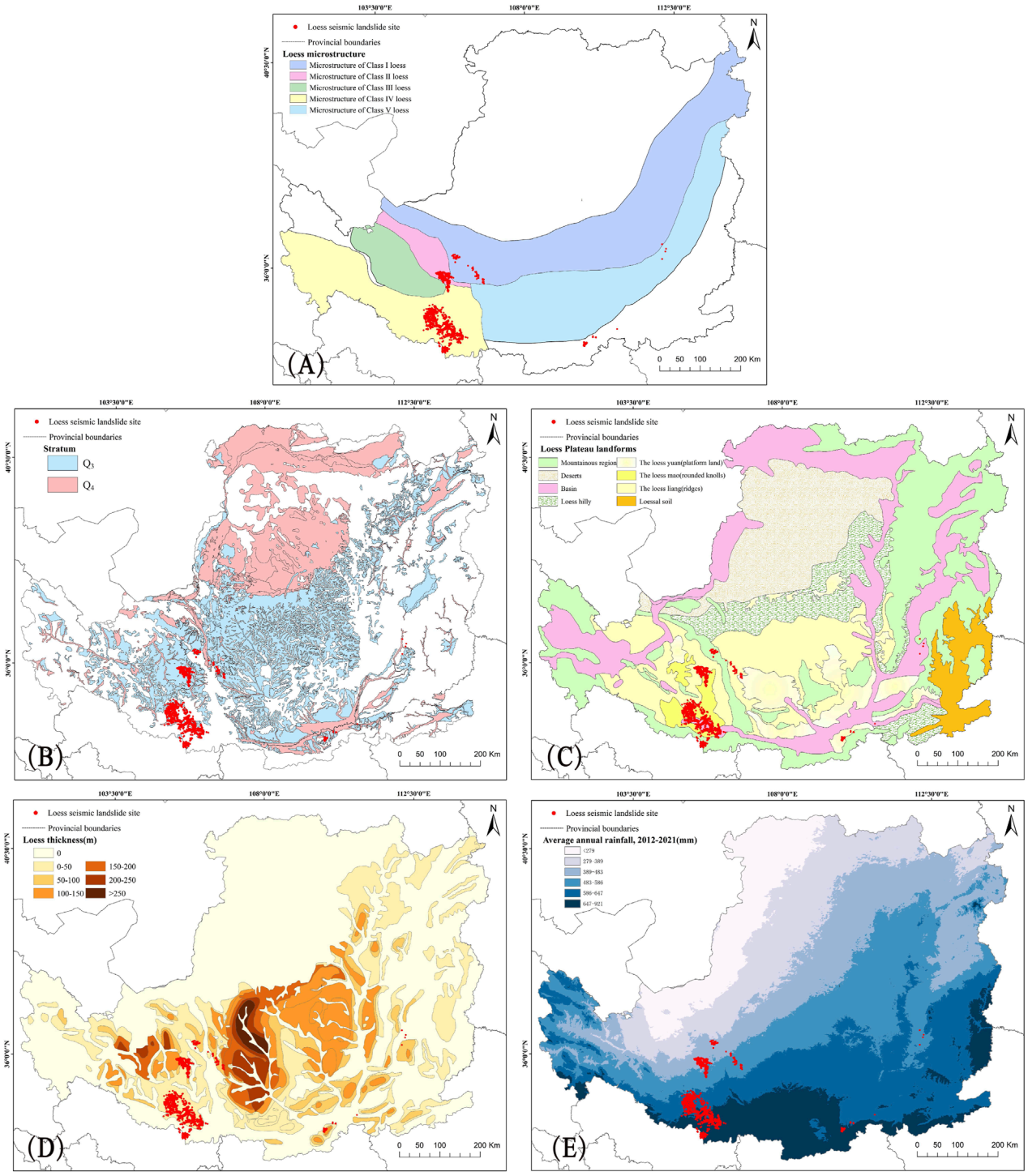

FIGURE 4
Impact factor: **(A)** Distribution of loess microstructure on the Loess Plateau. **(B)** Distribution of stratum on the Loess Plateau. **(C)** Distribution of landforms on the Loess Plateau. **(D)** Distribution of loess thickness on the Loess Plateau. **(E)** Distribution of average annual rainfall on the Loess Plateau, 2012–2021.

subsidence can occur rapidly even under relatively small saturation conditions (Fang et al., 2023).

The loess yuan (platform land), the loess mao (rounded knolls) and the loess liang (ridges) are the main landform types of the Loess Plateau (Figure 4C). Seismic subsidence mainly occurs in the loess yuan (platform land), terraces, the loess liang (ridges), and landslides mainly in the loess liang (ridges) and the loess mao (rounded knolls). Loess landslides occur in increasing order of occurrence in plains,

TABLE 2 Classification of loess microstructure types.

Microstructure type	I	II	III	IV	V
seismic subsidence coefficient	4–6.1%	1.5–5.5%	5–8%	1.5–3.68%	0.9–2%
cementation	weak	medium-strength	weak	agglomerated	medium-strength
pellets	sand based	powder based	macroporous	powder based	sticky grains predominate

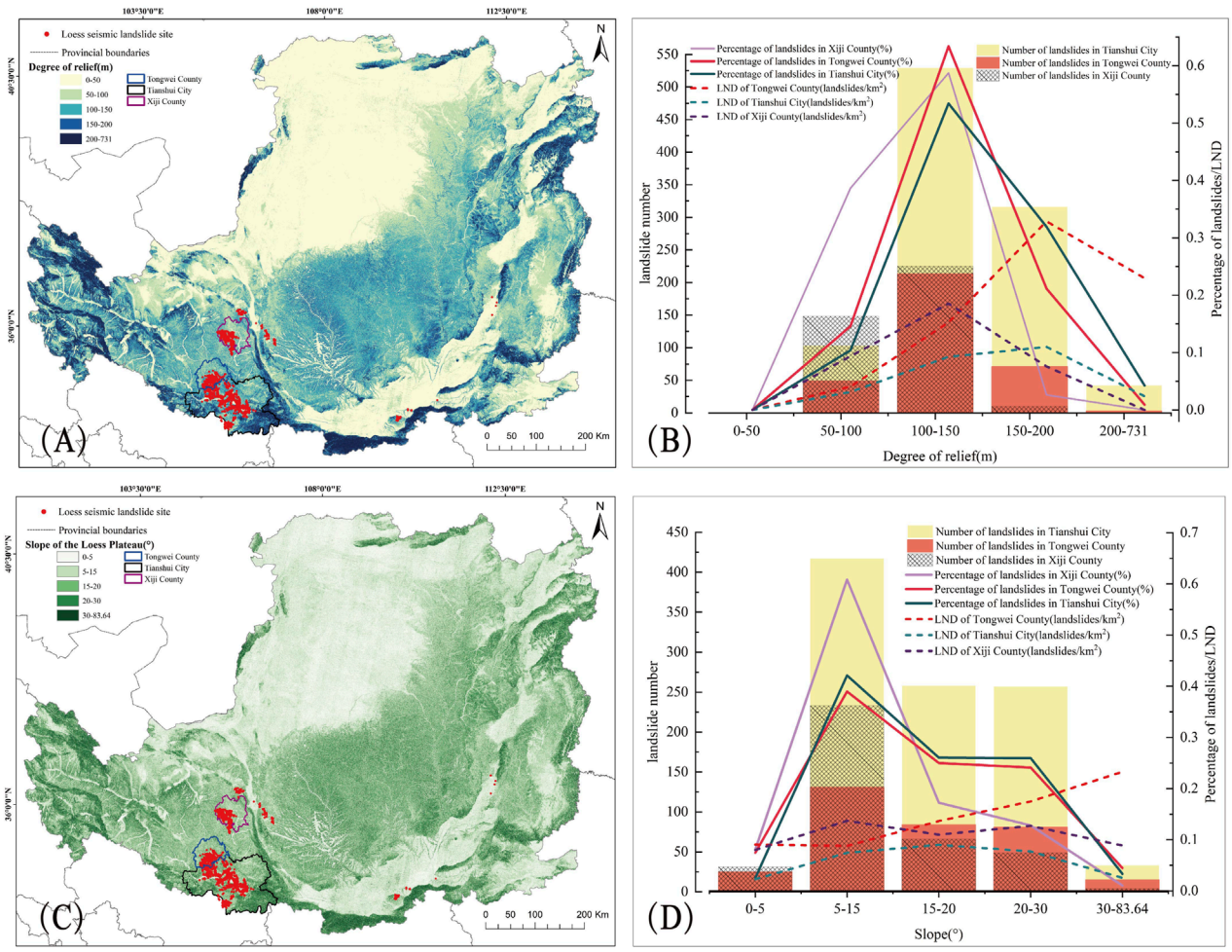

FIGURE 5
Degree of relief and slope analysis: **(A)** Distribution of degree of relief on the Loess Plateau analysis. **(B)** Degree of relief vs. percentage of seismically induced landslides vs. LND analysis map. **(C)** Distribution of slope on the Loess Plateau analysis. **(D)** Slope vs. seismic induced landslide percentage vs. LND analysis map.

alpine and hilly landscapes (Qiu et al., 2017). At the same time, loess topography has an amplifying effect on the ground motion of the site: under the loess yuan (platform land), acceleration, velocity, and displacement show an amplification effect with increasing elevation, and the maximum ground acceleration peak occurs at the leading edge of the hilltop. The peak ground acceleration of the loess liang (ridges) slope site shows the distribution pattern that the top of the slope is larger than the waist of the slope, and the waist of the slope is larger than the foot of the slope.

3.6 Loess thickness

Loess seismic landslides are concentrated in the loess thickness range of 25–35 m (Jie, 2017). Meanwhile, the thickness of loess cover has an amplifying effect on ground motion, loess overburden magnifies the seismic intensity at the top of the mountain by 1–2° compared to the bottom of the mountain (Wang et al., 2019). According to the study on the spatial distribution of loess thickness on the Loess Plateau conducted by the Institute of

TABLE 3 FR model values for rainfall impact factors.

Factor	Class	No. of landslides	Domain (km^2)	Percentage of landslides	Percentage of area	FR	Normalized class
Average annual rainfall 2012–2021 (mm)	<389	0	168,323.72	0.00	0.27	0.00	0.00
	389–483	379	125,018.24	0.19	0.20	0.97	0.33
	483–596	204	130,545.03	0.10	0.21	0.50	0.17
	596–647	743	132,832.26	0.38	0.21	1.79	0.60
	647–921	631	67,921.95	0.32	0.11	2.97	1.00

Earth Environment, Chinese Academy of Sciences (ENGLISH), the distribution of the thickness of loess cover on the Loess Plateau was extracted from the ArcGIS platform (Figure 4D).

3.7 Average annual rainfall

Timing of landslides coincides with, or slightly lags behind, rainfall distribution. Under the influence of rainfall, the water content of loess increases and the shear strength of loess decreases sharply (Derbyshire et al., 1994). At the same depth, loess subsidence increases with increasing water content (Yang et al., 2020). The average annual rainfall of the Loess Plateau from 2012 to 2021 (Figure 4E) was selected, and the frequency ratio (FR) model was applied to calculate the probability of occurrence of earthquakes on the Loess Plateau at different intervals. (Table 3).

3.8 Factor quantification and grading

The seismic-collapsed loess landslides are one of the types of loess seismic landslides, which are induced by the uneven settlement caused by loess subsidence. Referring to the influence factors of loess seismic landslides, and the segmental hazards, combined with the special microstructure of loess and loess subsidence characteristics, the integrated minimum hazard-causing seismic peak ground acceleration is the zoning method, and the evaluation factors are assigned in segments (Table 4).

4 The analytic hierarchy process to obtain the weights

The analytic hierarchy process (AHP) can organically combine qualitative and quantitative methods, with relatively few requirements for quantitative data, and is suitable for the current lack of a complete database of seismic-collapsed loess landslides. By constructing the relative importance matrix and multiplying it with the guideline layer vector to obtain the weighting matrix, and passing the consistency test, the evaluation results are more reasonable.

4.1 Constructing a hierarchical model of evaluation factors

A hierarchical model is constructed by combining the selected factors with the target layer. The assessment of the risk of seismic-collapsed loess landslides on the Loess Plateau is the target layer, and the evaluation factors are the programme layer.

4.2 Constructing judgement matrix and obtaining evaluation factor weights

Table 5 shows the qualitative descriptors for the comparison of impact factors in the indicators of the evaluation system. The weight of each evaluation factor was obtained by comparing the evaluation factors two by two and constructing a matrix (Table 6). The final result of obtaining the weight of each evaluation factor is: sesmic peak ground acceleration 0.4294; loess microstructure 0.1891; landform 0.1329; slope 0.0968; loess thickness 0.0609; stratum 0.0413; average annual rainfall 0.0277; degree of relief 0.0219. Also CR=0.0471<1, which passes the consistency test.

5 Discussion

The seismic-collapsed loess landslides are induced by earthquakes to damage loess structures and produce uneven settlement of the ground, thus inducing the occurrence of landslides. Among the many factors affecting seismic-collapsed loess landslides, earthquake is the main inducing factor and the rest are influencing factors. The hazard of seismic-collapsed loess landslides is analysed for different exceedance probabilities as follows.

5.1 Frequent ground motion

In the zoning map of frequent ground motion parameters, 0.1 g of ground acceleration is required to produce class I seismic subsidence. Additionally, 0.2 g of seismic peak ground acceleration is required to produce seismic-collapsed loess landslides, which is a very small percentage of the total. The probability of

TABLE 4 Evaluation indicator classification table.

Indicator	Class	Score	Indicator	Class	Score
Minimum hazard-causing seismic PGA (g)	PGA<0.1 g	0	Average annual rainfall of 2011–2021(mm)	<389	0
	0.1 g≤PGA<0.2 g	2		389–483	2
	0.2 g≤PGA<0.4 g	3		483–596	1
	0.4 g≤PGA<0.8 g	4		596–647	3
	0.8 g≤PGA<1.2 g	5		647–921	4
	PGA≥1.2 g	6	Loess thickness (m)	no loess cover	0
Loess microstructure	I	4		0–50	2
	II	3		>50	1
	III	5	Stratum	Q_3、Q_4	2
	IV	2		other	0
	V	1	Slope(°)	0–5	1
Degree of relief (m)	0–50	1		5–15	4
	50–100	3		15–20	3
	100–150	5		20–30	2
	150–200	4		30–83.64	1
	200–731	2			
Landform	desert	0			
	the loess yuan, liang,mao	3			
	loess hilly	2			
	mountains region	1			

TABLE 5 Scale of judgment matrix and its meaning.

Scale value	Connotation
1	two factors are of equal importance compared to each other
3	the former is slightly more important than the latter
5	the former is significantly more important than the latter
7	the former is strongly more important than the latter
9	the former is extremely more important than the latter
2,4,6,8	intermediate values of the above adjacent judgements
1/I (i=1,2, …,9)	contrary to the effects described above

occurrence of seismic-collapsed loess landslides under frequent ground subsidence is small, and in the current statistics, it rarely occurs under the condition of frequent ground motion.

5.2 Basic ground motion

Under the basic seismic peak ground acceleration, seismic-collapsed loess landslides on the Loess Plateau are divided into four hazard classes, which are no-risk, low-risk zone, moderate-risk zone, and relatively high-risk zone (Figure 6A). The no-risk zone that does not produce seismic-collapsed loess landslides, some areas with seismic peak ground acceleration at 0.05 g, and some areas with no loess-covered areas, such as the Mao Wusu Desert, do not involve loess subsidence phenomena. Huachi County, Zhidan County, etc., is a low-risk area, mainly because of the special geomorphological type of the loess liang (ridges) in this area, the top of the loess liang (ridges) on the ground motion acceleration amplification factor, up to 1.5–2 times. Relatively high-risk zone are located in Haiyuan County and Xiji County. The 5.8 magnitude earthquake that occurred in Yongdeng County in 1995 generated a large number of loess subsidence phenomena in the seismic area. Near the GeTa village in Yongdeng County, seismic-collapsed loess landslides occurred, with the maximum peak ground acceleration

TABLE 6 Evaluation indicator classification table.

Indicator	PGA	Loess microstructure	degree of relief	Slope	Landform	Loess thickness	Stratum	Average annual rainfall
PGA	1	4	9	6	5	7	8	9
loess microstructure	0.25	1	6	3	2	4	5	6
degree of relief	0.1111	0.1667	1	0.2	0.1667	0.25	0.3333	0.5
slope	0.1667	0.3333	5	1	0.5	2	3	6
landform	0.2	0.5	6	2	1	3	4	5
loess thickness	0.1429	0.25	4	0.5	0.3333	1	2	3
stratum	0.1250	0.2	3	0.3333	0.25	0.5	1	2
average annual rainfall	0.1111	0.1667	2	0.1667	0.2	0.3333	0.5	1

in the seismic zone ranging from 0.15g to 0.16g (Chen et al., 2000), consistent with the minimum hazard-causing seismic peak ground acceleration in Yongdeng County under the basic ground motion. There is good agreement with the classification of this area as a moderate and relatively-high risk zone in the results of this paper, indicating the soundness of the methodology.

5.3 Rare ground motion

Under the rare ground motion, the seismic-collapsed loess landslides on the Loess Plateau were classified into five risk levels, which were no-risk zone, low-risk zone, moderate-risk zone, relatively high-risk zone, and high-risk zone (Figure 7). The area of the no-risk zone is about 86,361 km^2, accounting for 13.83 percent of the area of the Loess Plateau. The area of the low-risk zone is about 148,116 km^2, accounting for 23.71 percent of the area of the Loess Plateau. The area of the moderate-risk zone is about 287,018 km^2, accounting for 45.95 percent of the area of the Loess Plateau. The area of the relatively high-risk zone is about 94,673 km^2, accounting for 15.16 percent of the area of the Loess Plateau. The high-risk area is about 8,490 km^2, accounting for 1.36 percent of the area of the Loess Plateau. The proportion of moderate-to high-risk areas reached 62.47 percent.

At 23:59 of 18 December 2023, a strong earthquake with a magnitude of M6.2 with a focal depth of 10 km struck Jishishan County in Gansu Province, China (Wang et al., 2024; Yang et al., 2024). The earthquake was the largest earthquake to hit mainland China in 2023 and killed 151 people. The seismic subsidence site (Figure 8A) was found within the seismic intensity VI. This produced a large number of ground fissures on the ground surface (Figure 8B, 9B), damaging both roads (Figure 8E) and generating landslide phenomenon (Figures 8C, 9C), which further impacted the local photovoltaic power generation site (Figure 8D), resulting in a huge economic loss. It is in good conformity with this paper to classify this area as a relatively high-risk area (Figure 7).

Schematic diagram of a seismic-collapsed loess landslide (i.e., Figure 9A) based on the terrain section line (i.e., red line) in Figure 9C. There are two main subsidence sliding surfaces at the subsidence site. Between the two major subsidence sliding surfaces, deformation was predominantly vertical, and a large number of ground fissures were generated. Horizontal deformation dominates below the lower subsidence slip surface. The reason for the more serious damage between the two seismic slip surfaces is the amplification effect of the topography on the ground motion of the site. Its formation by: the top of the slope and the upper part of the slope significant seismic amplification effect, first of all, will make the upper part of the slope loess pore structural damage → significant residual strain generation → uneven soil subsidence fall → the back of the slope to produce tensile fissure → slope in the middle and lower part of the soil by the upper part of the loess subsidence of the soil additional load and seismic inertial force and the joint action of the short-range shear slip out of the upper part of the soil body subsidence.

5.4 Very rare ground motion

Under the very rare ground motion, the loess plateau seismic-collapsed loess landslides are divided into six hazard classes, which are no-risk zone, low-risk zone, moderate-risk zone, relatively high-risk zone, high-risk zone and extremely high-risk zone (Figure 6B). The no-risk area is mainly desert-covered area, and there is no low-risk area, the moderate-risk area covers about 240,331 km^2, accounting for 38.55% of the total area of the Loess Plateau. The

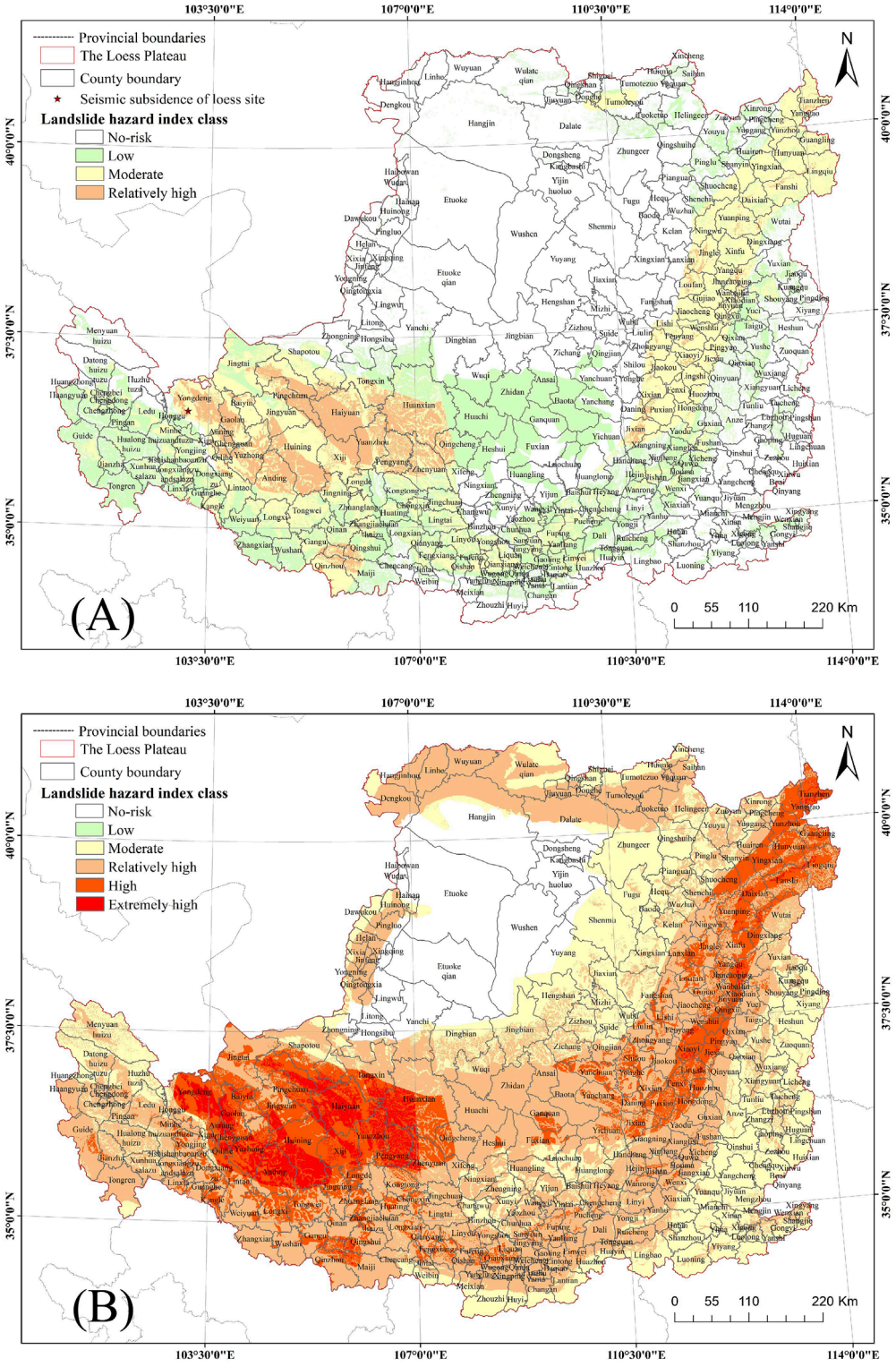

FIGURE 6
Seismic-collapsed loess landslides hazard risk zoning map: **(A)** Seismic-collapsed loess landslides hazard risk zoning map of basic ground motion on the Loess Plateau. (50-year exceedance probability 10 percent) and **(B)** Seismic-collapsed loess landslides hazard risk zoning map of very rare ground motion on the Loess Plateau. (50-year exceedance probability 0.5 percent).

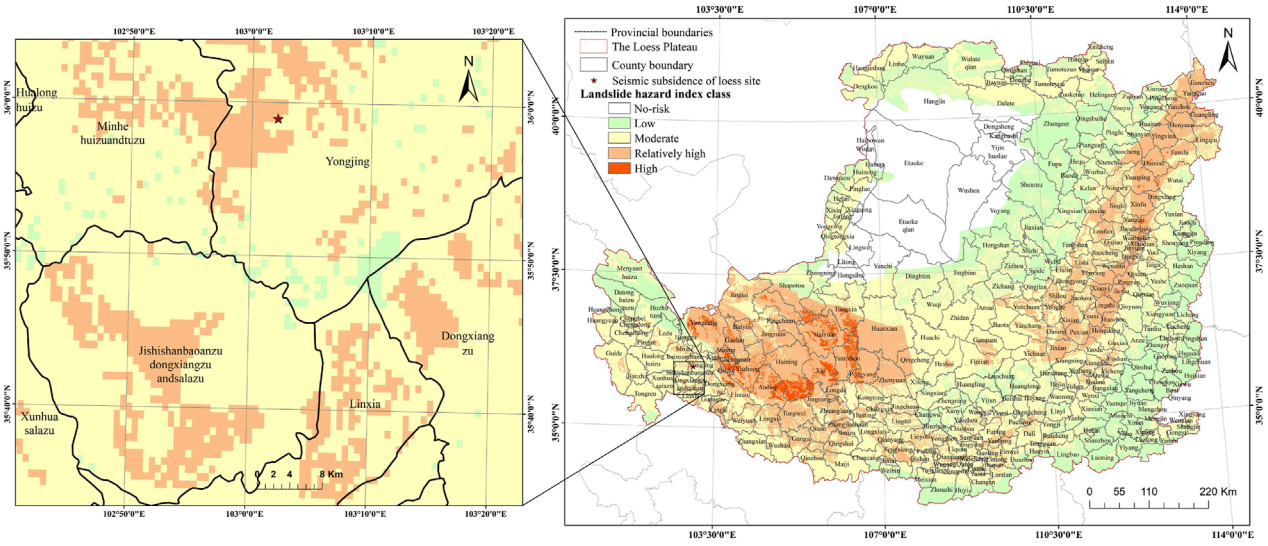

FIGURE 7
Seismic-collapsed loess landslides hazard risk zoning map of rare ground motion on the Loess Plateau. (50-year exceedance probability 2 percent).

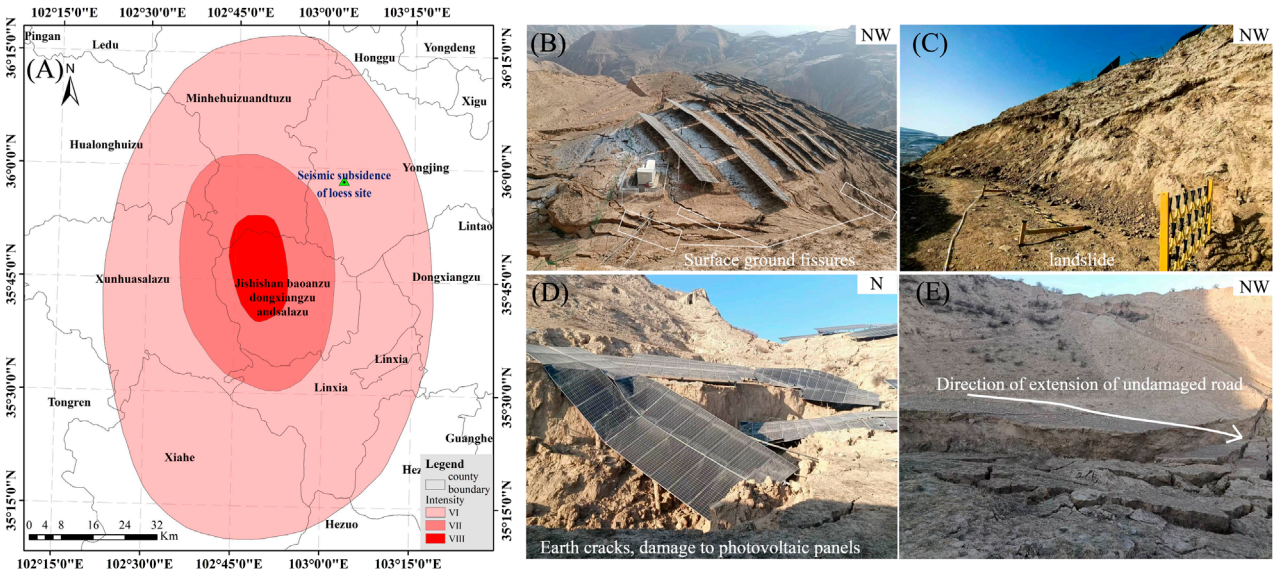

FIGURE 8
Location map and overview of the seismic subsidence field area: **(A)** Location map of the subsidence field area. **(B)** Surface ground fissures. **(C)** Landslide. **(D)** Destruction of photovoltaic panels. **(E)** Partial destruction of roads by ground fissures.

relatively high-risk area covers about 208,956 km^2, accounting for 33.51% of the total area of the Loess Plateau. The high-risk area covers about 69, 942 km^2, accounting for 11.22% of the total area of the Loess Plateau. The area of extremely high-risk zone is about 19, 922 km^2, accounting for 3.2% of the total area of the Loess Plateau. The proportion of relatively high-risk zones and above is about 50 percent. The M_s 8.5 earthquake in Haiyuan in 1920 was one of the largest and most destructive intraplate earthquakes in the early 20th century (Xu et al., 2019). It triggered large-scale landslides in Guyuan City, Xiji County, Huining County, Jingning County, Tongwei County, and other areas (Zhuang et al., 2018). A considerable number of loess seismic landslides occurred in Xiji County, which lies within the IX and X intensity zones of this earthquake. A typical seismic-collapsed loess landslide was discovered in Chuanerli of the county (Wang et al., 2023). In the zoning results shown in Figure 6B, Xiji County as a whole is classified as high and extremely high-risk areas, which align well with the actual situation.

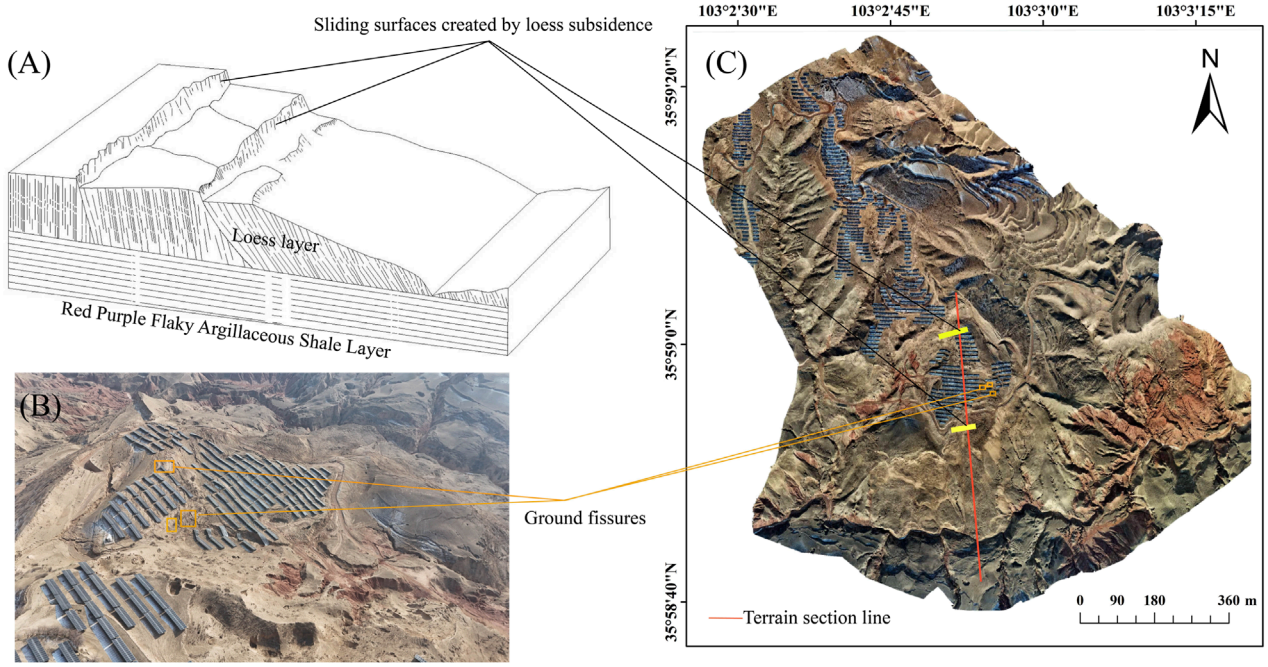

FIGURE 9
Schematic diagram of UAV remote sensing imagery and topographic County: **(A)** Schematic diagram of seismic-collapsed loess landslides. **(B)** Overview map between two seismic subsidence sliding surfaces. **(C)** Remote sensing image of seismic-collapsed loess landslides in loess subsidence.

6 Conclusion

Combining the characteristics of loess subsidence and the factors influencing loess seismic landslides, eight factors are selected. These factors are combined with the minimum hazard-causing seismic peak ground acceleration and the analytic hierarchy process method. Consequently, the seismic-collapsed loess landslides hazard assessment map is plotted under different exceedance probabilities. The case of seismic-collapsed loess landslides induced by the M6.2 magnitude earthquake in Jishishan County, China, is presented as an important illustration validating the zoning results. The following conclusions were obtained:

(1) Loess seismic landslides have the highest number of distributions on slopes of 5°–15°, and fewer distributions on slopes of 0°–5° and >30°, i.e., the slopes are particularly gentle and too steep, with fewer landslide disasters. The degree of relief of the Loess Plateau is within the range of 0–731 m. Within the degree of relief of 100–150 m, loess seismic landslides are more distributed.

(2) The minimum hazard-causing seismic peak ground acceleration is the inducing factor and the rest are the influencing factors in the index system of seismic-collapsed loess landslides on the Loess Plateau. Loess microstructure has the highest weight in the influence factors.

(3) The formation mechanism of the loess seismic subsidence site generated by the M6.2 magnitude earthquake in Jishishan, Gansu Province, China, is consistent with the basic law of seismic-collapsed loess landslides formation. It matches well with this study's classification of it as a relatively high-risk area. The degree of damage is greater than the top of the slope than the waist of the slope than the foot of the slope. In the study, it is found that the amplification effect of the site is difficult to be superimposed in the regional risk assessment, which is a place that still needs to be supplemented in the follow-up work.

(4) Under different exceedance probabilities, the probability of seismic-collapsed loess landslides is lower under the 50-year exceedance probability of 63%. With the increase of minimum hazard-causing seismic peak ground acceleration, the risk of occurrence of seismic-collapsed loess landslides rises, and the proportion of the area of moderate-high risk zone gradually expands.

(5) The results of the hazard assessment are in good conformity with the existing data of seismic-collapsed loess landslides, which can provide a reference for disaster prevention and mitigation in the Loess Plateau. The combination of the minimum hazard-causing seismic peak ground acceleration method and the analytic hierarchy process method can provide a reference for the assessment of geological hazards with earthquake as the main inducing factor and the rest of the influencing factors.

Data availability statement

The original contributions presented in the study are included in the article/Supplementary Material, further inquiries can be directed to the corresponding author.

Author contributions

YW: Formal Analysis, Writing–original draft. PW: Methodology, Project administration, Writing–original draft. WC: Investigation, Writing–original draft. HW: Investigation, Writing–original draft. SgX: Investigation, Writing–review and editing. SaX: Investigation, Writing–original draft. HY: Writing–original draft, Writing–review and editing.

Funding

The author(s) declare financial support was received for the research, authorship, and/or publication of this article. This research was funded by the following grants: Science for Earthquake Resilience (XH23041C); Science for Earthquake Resilience (XH23043YA); National Natural Science Foundation of China (NSFC)(U1939209); Centre for Physical Exploration Youth Fund(YFGEC2022006); The Natural Science Foundation of Gansu Province (Grant No.22JR11RA091).

Acknowledgments

We are grateful to the Institute of disaster prevention for providing the loess seismic landslides data, to PW for his careful teaching, and to the subject group for their joint help.

Conflict of interest

The authors declare that the research was conducted in the absence of any commercial or financial relationships that could be construed as a potential conflict of interest.

The reviewer AX declared a shared affiliation with the author WC to the handling editor at time of review.

Publisher's note

Supplementary material

The Supplementary Material for this article can be found online at: https://www.frontiersin.org/articles/10.3389/feart.2024.1402922/full#supplementary-material

References

Aditian, A., Kubota, T., and Shinohara, Y. (2018). Comparison of GIS-based landslide susceptibility models using frequency ratio, logistic regression, and artificial neural network in a tertiary region of Ambon, Indonesia. *Geomorphology* 318, 101–111. doi:10.1016/j.geomorph.2018.06.006

Basu, T., and Pal, S. (2017). Exploring landslide susceptible zones by analytic hierarchy process (AHP) for the Gish River Basin, West Bengal, India. *Spat. Inf. Res.* 25 (5), 665–675. doi:10.1007/s41324-017-0134-2

Bui, D. T., Lofman, O., Revhaug, I., and Dick, O. (2011). Landslide susceptibility analysis in the Hoa Binh province of Vietnam using statistical index and logistic regression. *Nat. Hazards* 59 (3), 1413–1444. doi:10.1007/s11069-011-9844-2

Chen, Y., Shi, Y., Xu, H., and Liu, H. (2000). Characteristics of Seismic subsidence of loess deformation and its formation mechanism in the 1995 Yongdeng earthquake. *Northwest. Seismol. J.* 22 (4), 465–470. (in Chinese).

Deng, J., Wang, L., Zhang, Z., Sun, J., and Zhong, X. (2003). The China loess microstructure types and its seismic subsidence zones divided. *China Earthq. Eng. J.* 35 (03), 664–670. (in Chinese).

Derbyshire, E., Dijkstra, T. A., Smalley, I. J., and Li, Y. (1994). Failure mechanisms in loess and the effects of moisture content changes on remoulded strength. *Quat. Int.* 24, 5–15. doi:10.1016/1040-6182(94)90032-9

Duan, R., and Zhang, Z. (1990). Further studies on the dynamic properties of loess. *China Earthq. Eng. J.* 12 (03), 72–78. (in Chinese).

Fang, R., Zhang, S., Deng, L., Fan, W., and Wang, H. (2023). Research on a classification model of loess seismic landslides based on random forest in the Haiyuan region. *Bull. Eng. Geol. Environ.* 82, 72. doi:10.1007/s10064-023-03096-5

Guo, Z., Huang, Q., Liu, Y., Wang, Q., and Chen, Y. (2023). Model experimental study on the failure mechanisms of a loess-bedrock fill slope induced by rainfall. *Eng. Geo* 313, 106979. doi:10.1016/j.enggeo.2022.106979

Jie, J. (2017). *Hazard evaluation of strong earthquake loess landslides in high intensity mountainous areas*. Master's thesis. China: Chengdu University of Technology.

Jin, K. P., Yao, L. K., Cheng, Q. G., and Xing, A. G. (2019). Seismic landslides hazard zoning based on the modified Newmark model: a case study from the Lushan earthquake, China. *Nat. Hazards* 99 (1), 493–509. doi:10.1007/s11069-019-03754-6

Li, K., Xu, C., Tan, M., Chen, J., Li, S., Luo, J., et al. (2019). Gis-Based and logistic regression model for hazard assessment of landslides triggered by hejing earthquake in 2012. *JEG* 27 (S1), 262–268. doi:10.13544/j.cnki.jeg.2019102

Li, X., Yan, L., Wu, Y., Peng, D., Duan, J., and Bo, J. (2023). Distribution and characteristics of loess landslides induced by the 1654 Tianshui earthquake, Northwest of China. *Landslides* 20, 2775–2790. doi:10.1007/s10346-023-02128-1

Li, Y., Ming, D., Zhang, L., Niu, Y., and Chen, Y. (2024). Seismic landslide susceptibility assessment using Newmark displacement based on a dual-channel convolutional neural network. *Remote Sens.* 16 (3), 566. doi:10.3390/rs16030566

Myronidis, D., Papageorgiou, C., and Theophanous, S. (2016). Landslide susceptibility mapping based on landslide history and analytic hierarchy process (AHP). *Nat. Hazards* 81 (1), 245–263. doi:10.1007/s11069-015-2075-1

Newmark, N. M. (1965). Effects of earthquakes on dams and embankments. *Geotechnique* 15 (2), 139–160. doi:10.1680/geot.1965.15.2.139

Peng, J. (2019). *Landslide disaster in loess Plateau*. Chinese, Beijing: Science Press.

Pu, X., and Xu, S. (2019). Characteristics and mechanism of loess landslides induced by strong earthquake in the Loess Plateau of China. *IOP Conf. Ser. Earth Environ. Sci.* 332 (2), 022025–25. doi:10.1088/1755-1315/332/2/022025

Qian, Z. (2023). *Evaluation of the risk of loess earthquake landslides based on the statistical model*. Master's thesis. China: Lanzhou Institute of Seismology, CEA.

Qiu, H., Regmi, A. D., Cui, P., Hu, S., Wang, Y., and He, Y. (2017). Slope aspect effects of loess slides and its spatial differentiation in different geomorphologic types. *Arab. J. Geosci.* 10 (15), 344–2709. doi:10.1007/s12517-017-3135-5

Qiu, J., Wang, X., Lai, J., Zhang, Q., and Wang, J. (2018). Response characteristics and preventions for seismic subsidence of loess in Northwest China. *Nat. Hazards Rev.* 92 (3), 1909–1935. doi:10.1007/s11069-018-3272-5

Roslee, R., Micke, A., Simon, N., and Norhisham, M. N. (2017). Landslide susceptibility analysis LSA using weighted overlay method WOM along the genting sempah to bentong highway pahang. *MJG* 1 (2), 13–19. doi:10.26480/mjg.02.2017.13.19

Runde, L., Hongru, Z., Xiaohong, B., Rengwang, L., and Fengxiang, Y. (2007). Dynamic shear strength and seismic subsidence of intact loess with different water contents from dynamic triaxial testing. *JEG* 15, 694–699. doi:10.3969/j.issn.1004-9665.2007.05.019

Shahabi, H., Ahmadi, R., Alizadeh, M., Hashim, M., Al-Ansari, N., Shirzadi, A., et al. (2023). Landslide susceptibility mapping in a mountainous area using machine learning algorithms. *Remote Sens.* 15 (12), 3112. doi:10.3390/rs15123112

Shi, Y., and Qiu, G. (2011). Constitutive relation of seismic subsidence of loess based on microstructure. *Chin. J. Geotechnical Eng.* 33 (S1), 7–11. (in Chinese).

Sun, Q., Zhang, T., Wang, H., Wu, j., Wang, H., Zhu, Y., et al. (2021). Application of shallow landslide stability model to landslide prediction in the Linxi River basin of southern Zhejiang. *East China Geol.* 42 (4), 383–389. doi:10.16788/j.hddz.32-1865/P.2021.04.003

Tian, Y., Xu, C., Xu, X., and Chen, J. (2016). Detailed inventory mapping and spatial analyses to landslides induced by the 2013 Ms 6.6 Minxian earthquake of China. *J. Earth Sci.* 27 (6), 1016–1026. doi:10.1007/s12583-016-0905-z

Wang, L. (2003). *Loess dynamics*. Chinese, Beijing: Seismological Press.

Wang, L. (2020). Mechanism and risk evaluation of sliding flow triggered by liquefaction of loess deposit during earthquakes. *Chin. J. Geotech.* 42 (1), 1–19. doi:10.11779/CJGE202001001

Wang, L., Chai, S., Bo, J., Wang, P., Xu, S., Li, X., et al. (2023). Triggering types, characteristics and disaster mechanism of seismic loess landslides. *Chin. J. Geotech. Eng.* 45 (8), 1543–1554. doi:10.11779/CJGE20220531

Wang, L., and Deng, J. (2023). The loess microstructure kinds and its seismic subsidence. *NS* 5 (07), 792–795. doi:10.4236/ns.2013.57095

Wang, L., Wu, Z., and a, K. (2017). Effects of site conditions on earthquake ground motion and their applications in seismic design in loess region. *J. Mt. Sci.* 14, 1185–1193. doi:10.1007/s11629-016-3921-7

Wang, L., Wu, Z., a, K., Liu, K., Wang, P., Pu, X., et al. (2019). Amplification of thickness and topography of loess deposit on seismic ground motion and its seismic design methods. *Soil Dyn.* 126, 105090. doi:10.1016/j.soildyn.2018.02.021

Wang, L., Xu, S., Wang, P., Wang, R., Che, A., Zhou, Y., et al. (2024). Characteristics and lessons of liquefaction-triggered large-scale flow slide in loess deposit during Jishishan M6.2 earthquake in 2023. *Chin. J. Geotechnical Eng.* 46 (2), 235–243. doi:10.11779/CJGE20240038

Wang, N., Wang, L., Yuan, Z., and Wang, Q. (2012). Characteristic and stability analysis for loess seismic landslide in valley city. *Adv. Mat. Res.* 594-597, 1856–1863. doi:10.4028/scientific.net/AMR.594-597.1856

Wang, P. (2022). *Disaster-causing mechanism of loess subsidence in unsaturated loess and its evaluation scheme*. Dissertation thesis. China: Xi'an University Of Technology.

Wang, Y., Wang, L., and Zhang, X. (2004). GIS-supported seismic landslide zoning study on the Loess Plateau. *J. Geogr.* 24 (2), 170–176. doi:10.3969/j.issn.1000-0690.2004.02.007

Xing, X., Li, T., and Fu, Y. (2016). Determination of the related strength parameters of unsaturated loess with conventional triaxial test. *Environ. Earth Sci.* 75 (1), 82. doi:10.1007/s12665-015-4797-5

Xu, P., Zhang, Q., Qian, H., Li, M., and Yang, F. (2021). An investigation into the relationship between saturated permeability and microstructure of remolded loess: a case study from Chinese Loess Plateau. *Geoderma* 382 (0016-7061), 114774. doi:10.1016/j.geoderma.2020.114774

Xu, X., Zhang, Z., Hu, F., and Chen, X. (2019). Dynamic rupture simulations of the 1920 MS 8.5 Haiyuan earthquake in China. *B Seismol. Soc. Am.* 109 (5), 2009–2020. doi:10.1785/0120190061

Yang, W., Pan, B., Jin, L., Wang, Y., and Saleem, F. (2020). Experimental study on dynamic characteristics of Qingyang loess under different water contents. *Arab. J. Geosci.* 13 (19), 986. doi:10.1007/s12517-020-05989-1

Yang, Z. G., Liu, J., Zhang, Y. Y., Yang, W., and Zhang, X. M. (2024). Rapid report of source parameters of 2023 M6.2 Jishishan, Gansu earthquake sequence. *Earth Planet. Phys.* 8 (2), 436–443. doi:10.26464/epp2024012

Zang, M., Qi, S., Sheng, Z., Zamora, B. S., and Zou, Y. (2019). An improved method of Newmark analysis for mapping hazards of co-seismic landslides. *Nat. Hazards Earth Syst. Sci.* 20 (3), 1–44. doi:10.5194/nhess-2019-42

Zhang, J., Lin, C., Tang, H., Wen, T., Tannant, D. D., and Zhang, B. (2024b). Input-parameter optimization using a SVR based ensemble model to predict landslide displacements in a reservoir area–A comparative study. *Appl. Soft Comput.* 150, 111107. doi:10.1016/j.asoc.2023.111107

Zhang, J., Peng, J., Xu, C., and Li, Z. (2017). Distribution and characteristics of loess landslides triggered by the 1920 Haiyuan Earthquake, Northwest of China. *Geomor* 314, 1–12. doi:10.1016/j.geomorph.2018.04.012

Zhang, J., Tang, H., Li, C., Gong, W., Zhou, B., and Zhang, Y. (2024a). Deformation stage division and early warning of landslides based on the statistical characteristics of landslide kinematic features. *Landslides* 21, 717–735. doi:10.1007/s10346-023-02192-7

Zhang, M., and Li, T. (2011). Triggering factors and forming mechanism of loess landslides. *JoE* 19 (4), 530–540. doi:10.3969/j.issn.1004-9665.2011.04.014

Zhong, X., Xu, X., Chen, W., Liang, Y., and Sun, Q. (2022). Characteristics of loess landslides triggered by the 1927 Mw8.0 earthquake that occurred in Gulang county, Gansu province. *China. Front. Environ. Sci.* 10, 973262. doi:10.3389/fenvs.2022.973262

Zhuang, J., Peng, J., Xu, C., Li, Z., Densmore, A., Milledge, D., et al. (2018). Distribution and characteristics of loess landslides triggered by the 1920 Haiyuan Earthquake, Northwest of China. *Geomorphology* 314, 1–12. doi:10.1016/j.geomorph.2018.04.012